Massive Stars Across Redshifts in the Era of JWST and Large Surveys
Proceedings IAU Symposium No. 402, 2026
A. Wofford, N. St Louis, M. García, S. Simón-Díaz & L. M. Oskinova, eds.
doi:10.1017/S1743921326105596

A new generation of empirical metallicity calibrations based on a comprehensive T_e-based approach for local and high-redshift studies

F. Fabián Rosales-Ortega[1], J. Eduardo Méndez-Delgado[2] and the DESIRED team

[1]Instituto Nacional de Astrofísica, Óptica y Electrónica (INAOE SECIHTI), Luis E. Erro 1, 72840, Tonantzintla, Puebla, México;
email: frosales@inaoep.mx

[2]Instituto de Astronomía, Universidad Nacional Autónoma de México, A.P. 70-264, 04510 CDMX, México

Abstract. We present a new generation of optical strong-line metallicity calibrations based on the most extensive compilation of abundances determined using electronic temperatures to date: over 2700 spectra of extragalactic HII regions and star-forming galaxies with auroral line detections from the DESIRED project. Unlike previous calibrations derived from small, heterogeneous datasets, our work applies strict quality criteria, propagates uncertainties, and accounts for temperature inhomogeneities, addressing the long-standing abundance discrepancy. The resulting calibrations refine and extend classical empirical indicators with unprecedented robustness and coverage across the metallicity-ionisation parameter space. They span a broader validity range than earlier relations and avoid the distortions common in small samples, an issue especially relevant when confronting recent JWST-based high-z calibrations. These results provide a solid framework for tracing galactic chemical enrichment and for reconciling empirical observations with theoretical models of star formation and feedback across cosmic time.

Keywords. Metallicity, calibrations, abundances, HII regions, galaxies

1. Introduction

Optical nebular emission lines are among the most widely used diagnostics of gas-phase metallicity in galaxies, as strong lines in this range are accessible from the ground and extensively sampled by large surveys. However, the auroral lines required for direct Te-based abundance determinations are intrinsically weak, limiting their use to a few hundred nearby galaxies and H II regions. This has motivated the development of *strong-line* calibrations, which rely on bright emission-line ratios, but existing calibrations are typically based on small, heterogeneous datasets, leading to inconsistencies at both low and high metallicities.

The aim of this work is to establish a new generation of optical strong-line calibrations derived from the most extensive, high-quality compilation of Te-based data to date: over 2700 star-forming galaxies and H II regions from the DESIRED project. By applying a homogeneous methodology, we refine previous calibrations and introduce six new relations, accounting for the first time, for observational uncertainties and temperature inhomogeneities.

© The Author(s), 2026. Published by Cambridge University Press on behalf of The International Astronomical Union.

https://doi.org/10.1017/S1743921326105596 Published online by Cambridge University Press

2. Calibration sample

This work is based on the latest compilation from the DESIRED project (DEep Spectra of Ionised REgions Database; Méndez-Delgado et al. 2023), a collaborative effort aimed at studying photoionised nebulae through homogeneous analyses of high-quality optical spectra. The full DESIRED sample includes 3154 extinction-corrected spectra of ionised regions collected from both dedicated observations and the literature, covering HII regions, local and high-z star-forming galaxies (SFGs), and planetary nebulae. All spectra contain at least one auroral-to-nebular line ratio of collisionally excited lines (CELs), such as [O III] $\lambda4363/\lambda5007$, [N II] $\lambda5755/\lambda6584$, [S III] $\lambda6312/\lambda9069$, enabling direct determinations of the electron temperature (T_e).

For calibration purposes we focus on a subsample of 2740 objects, restricted to extragalactic HII regions and SFGs (local and $z > 2$). Galactic HII regions, PNe, and peculiar nebulae were excluded due to potential aperture biases. Physical conditions and abundances were derived with PyNeb (Luridiana et al. 2015; Morisset et al. 2020), solving for electron density (n_e) and T_e using density-sensitive ratios and temperature-sensitive diagnostics, propagating uncertainties through Monte Carlo simulations. Ionic abundances (O^+, O^{2+}) were calculated under both the homogeneous temperature assumption ($t^2 = 0$) and accounting for temperature inhomogeneities ($t^2 > 0$; Peimbert 1967). Total oxygen abundances were obtained as the sum of the ionic abundances, neglecting the minor contributions of O^{3+}.

3. High-quality matters: beyond large numbers

Previous calibrations often relied on heterogeneous data, overlooking the critical role of high-quality data. In this work we impose strict selection criteria to ensure the robustness of the calibration sample. We exclude regions where auroral lines have relative errors above 40%, where nebular line ratios deviate by more than 20% from theoretical expectations, where the uncertainty in 12+log(O/H) exceeds 0.3 dex, or where the derived electron temperature is higher than 25,000 K, as such cases may indicate high-density conditions ($n_e > 1000$ cm^{-3}) where T_e diagnostics become unreliable.

Figure 1 presents examples of three metallicity calibrations derived from the DESIRED high-quality calibration sample. For each index, we report two calibrations: one based on the classical direct method ($t^2 = 0$, shown as a yellow-black dashed line) and another that incorporates the effect of temperature variations ($t^2 > 0$, yellow solid line). These relations can be directly compared with previous determinations in Fig. 2, where grey contours trace the distribution of calibration regions in the metallicity-index plane. The DESIRED sample spans the full range of line ratios observed in H II regions and star-forming galaxies, covering the broadest metallicity range ever derived from auroral lines (12+log(O/H) $\approx 6.8 - -9.0, t^2 = 0$).

In many cases, the validity range of the DESIRED calibrations exceeds that of earlier relations based on smaller datasets. This wider coverage produces unusual shapes in some calibrations, particularly at the low- and high-metallicity ends. Such effects are especially relevant when comparing with calibrations derived from simulations (e.g., Hirschmann et al. 2023; Garg et al. 2024; Cornejo-Cárdenas et al. 2025) or with recent high-z calibrations based on several JWST sources (Chakraborty et al. 2025; Scholte et al. 2025; Sanders et al. 2025).

It is important to note that the present calibrations do not include corrections for the ionisation state of the gas (e.g., the ionisation parameter log u; or the P parameter, Pilyugin & Thuan 2005), nor do they account for variations in the specific star-formation rate (Curti et al. 2017). These aspects will be explored in a forthcoming publication.

https://doi.org/10.1017/S1743921326105596 Published online by Cambridge University Press

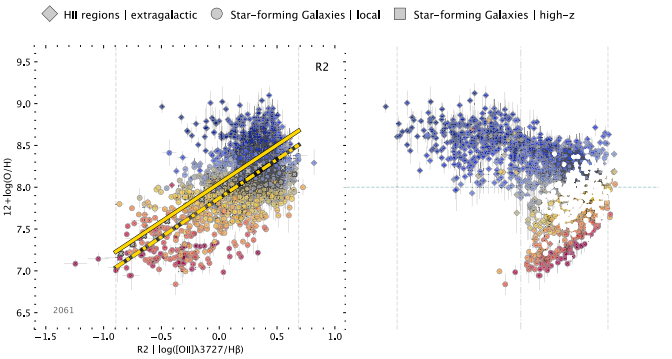


Figure 1. Example of 3 metallicity calibrations derived from the DESIRED high-quality calibration sample: R2, R3 and R23 calibrations. The notation and ratio indices are defined in the x-label of each panel. For monotonic relations (e.g., R2), the vertical grey dashed lines mark the validity range of each calibration; for bivalued relations (e.g., R23) they mark the validity range of the upper calibration branch, whereas the dashed-dotted line marks the minimum index validity value for the lower calibration branch. The horizontal blue dashed-line marks the separation between the lower and upper branch for bivalued calibrations. The regions are color-coded by their T_e in units of 10^4 K and their symbols correspond to the type of region as shown at the top of the figure. Error bars represent 1σ uncertainties. The value in the lower-left corner of each panel indicates the number of regions utilised for each calibration.

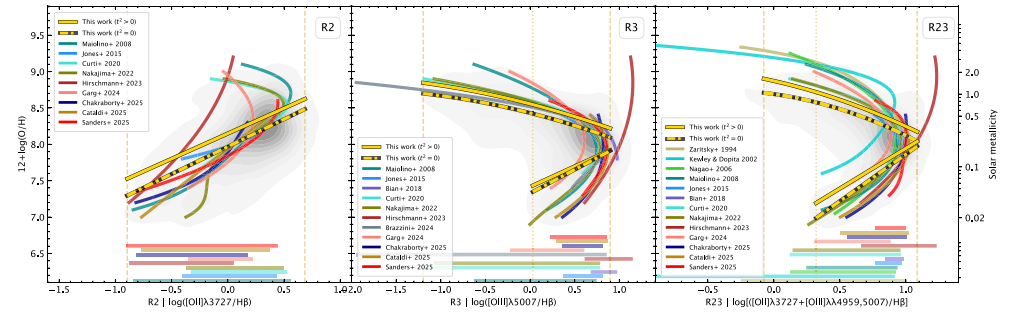


Figure 2. Comparison of the DESIRED metallicity calibrations with previous determinations from the literature for the calibrations shown in Fig. 1. Grey contours trace the density distribution of the calibration regions, derived from a kernel density estimation (KDE) and plotted at ten equally spaced probability levels, with darker shades indicating higher concentrations. The yellow-black dashed line and yellow solid line correspond to the $t^2 = 0$ and $t^2 > 0$ calibrations, respectively. Vertical yellow dashed lines mark the validity ranges of the DESIRED calibrations, while dotted lines indicate the minimum index value for the lower branch in bi-valued relations. Previous calibrations are shown as solid coloured lines, with references indicated in the legends. The horizontal coloured bars beneath each panel denote the validity ranges of each literature calibration.

References

Chakraborty, P., Sarkar, A., Smith, R., et al. 2025, ApJ, 985, 24
Cornejo-Cárdenas, A., Sillero, E., Tissera, P. B., et al. 2025, A&A, 699, A380
Curti, M., Cresci, G., Mannucci, F., et al. 2017, MNRAS, 465, 1384
Garg, P., Narayanan, D., Sanders, R. L., et al. 2024, ApJ, 972, 113
Hirschmann, M., Charlot, S., & Somerville, R. S. 2023, MNRAS, 526, 3504
Luridiana, V., Morisset, C., & Shaw, R. A. 2015, A&A, 573, A42

https://doi.org/10.1017/S1743921326105596 Published online by Cambridge University Press

Méndez-Delgado, J. E., Esteban, C., García-Rojas, J., Kreckel, K., & Peimbert, M. 2023, Nature, 618, 249
Morisset, C., Luridiana, V., García-Rojas, J., et al. 2020, Atoms, 8, 66
Peimbert, M. 1967, ApJ, 150, 825
Pilyugin, L. S., & Thuan, T. X. 2005, ApJ, 631, 231
Sanders, R. L., Shapley, A. E., Topping, M. W., et al. 2025, arXiv e-prints, arXiv:2508.10099
Scholte, D., Cullen, F., Carnall, A. C., et al. 2025, MNRAS, 540, 1800

https://doi.org/10.1017/S1743921326105596 Published online by Cambridge University Press